Superalloys 2008
Roger C. Reed, Kenneth A. Green, Pierre Caron, Timothy P. Gabb, Michael G. Fahrmann, Eric S. Huron and Shiela A. Woodard
TMS (The Minerals, Metals & Materials Society), 2008

MODELING TOPOLOGICALLY CLOSE-PACKED PHASES IN SUPERALLOYS: VALENCE-DEPENDENT BOND-ORDER POTENTIALS BASED ON AB-INITIO CALCULATIONS

T. Hammerschmidt, B. Seiser, R. Drautz, D. G. Pettifor

Materials Modelling Laboratory, Department of Materials, University of Oxford, United Kingdom

Keywords: bond-order potential, topologically close-packed phase, Re-W

Abstract

Refractory elements are used in Ni-based superalloys to increase creep resistance (Mo, Re, W) and to retard the coarsening of the γ' phase (Re). At high concentrations of refractory elements precipitation of topologically close-packed (*tcp*) phases [1] is detrimental to the creep properties of the alloys. A more detailed understanding of the formation kinetics and thermodynamic stability of *tcp* phases will therefore be beneficial for the design of the next generation superalloys. Atomistic modeling of *tcp* stability with interatomic potentials requires to go beyond the second-moment approximation to the electronic density of states by including up to at least the sixth moment [2]. We have developed an analytic bond-order potential (BOP) that systematically takes into account higher moment contributions to the density of states and depends explicitly on the valence of the transition-metal elements [3]. For the parameterization of the new BOP, we performed extensive density functional theory (DFT) calculations of elemental and binary compound phases of Ni, the technologically important alloying element Cr, and the refractory metals Mo, Re, and W. We will discuss the structural trends of the DFT calculations, compare to the predictions of the analytic BOP and report on our progress on the parameterization of the analytic BOP for the Re-W system. This work is part of the EPSRC-funded collaborative multi-scale project 'Alloys by Design'.

Introduction

Superalloys for commercial turbine blades have to fulfill stringent requirements on long-term stability at operating temperatures. In Ni-based superalloys, the mechanical properties are improved by adding molybdenum, rhenium, and tungsten. These refractory elements increase the creep resistance (Mo, Re, W) and retard the coarsening of the γ' phase (Re). At concentrations of the refractory elements of several weight percent, however, *tcp* phases precipitate [1] that are detrimental to the creep properties of the alloys. This upper bound for the concentration of refractory elements is a constraint in the design of the superalloy. It can also be exceeded due to interdiffusion at interfaces with coatings [4].

Topologically-closed packed phases are well known to form in compounds that contain transition metals. Their structures can be described in terms of networks of intersecting coordination polyhedra (see e.g. Sinha [5]). The coordination number (CN) of the central atom in these polyhedra ranges from 12 to 16 with an average value of more than 13 in the *tcp* phases. In this work we focus on those *tcp* phases that have been observed for binary transition-metal compounds: A15, C14, C15, C36, σ, μ, and χ. The structural stability of *tcp* phases is affected by electronegativity, differences in atomic-size and electronic structure effects (see e.g. Ref. [6] for a recent review on Laves phases). In many cases such effects can be identified in structure maps that are based on a one-dimensional ordering parameter for the elements, the so-called Mendeleev number $\mathcal{M}$ [7, 8] (see Fig. 1). The comparison of theoretically predicted structure maps with experimental data enables one to identify which effects dominate. Although density-functional theory (DFT) calculations can be routinely applied to determine formation energies with high accuracy, they are too computationally demanding to set up structure maps for all possible binary combinations of transition metals. The tight-binding method approximates the electronic density of states (DOS) and was proven to be sufficient to capture the experimentally observed structural trends [9]. In order to be able to understand the stability of *tcp* phases as a function of the local coordination, we require an approximation to the solution of the tight-binding model. We have presented a bond-order potential (BOP) that is an analytic expansion of the DOS in terms of moments [3]. This BOP depends explicitly on the valence of

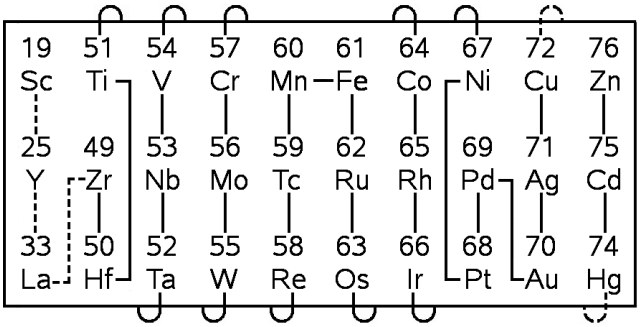

Figure 1: The Mendeleev number $\mathcal{M}$, here shown for the transition metals, is a one-dimensional ordering parameter for the elements of the periodic table [7, 8].

the transition-metal elements and reproduces the structural trend across the $4d$ and $5d$ transition-metal series. In this work we apply this BOP to the structural stability of *tcp* phases of binary transition-metal compounds.

In the first part of this paper we will present a phenomenological structure map of experimentally observed *tcp* phases in binary transition-metal compounds. The second part is devoted to density-functional theory calculations of the *tcp* phases in the binary systems Re-W, Mo-W and Mo-Re. In the last part we demonstrate that a recently developed analytic bond-order potential captures the trends of the structural stability of *tcp* phases.

Structure Map of *tcp* phases

The relative stability of *tcp* phases for binary transition-metal compounds is related to the average group number of the elements (see e.g. Ref. [5]). We have compiled a structure map of the occurrence of *tcp* phases for binary compounds from experimental databases that highlights not only this relationship, but also allows us to identify size effects. The data points of the structure map were collected from Pearson [10] and the Inorganic Crystal Structure Database (ICSD) [11]. These structures comprise ordered as well as disordered crystals that were observed at high as well as low temperatures. The average Mendeleev number of the compounds $\mathcal{M}_{AB}$ was determined from the average of the elemental Mendeleev numbers $\mathcal{M}_A$, $\mathcal{M}_B$ with weights according to the experimentally observed stoichiometry of the compound. The few cases with unknown chemical composition (e.g. Ta-V) were assumed to have a compound ratio of 1:1.

Crystal Structures

The *tcp* phases are made up of different combinations and mutual arrangements of coordination polyhedra as elemental formation units. The coordination polyhedra CN12 to CN16 that form the *tcp* phases A15, C14, C15, C36, σ, μ, and χ are shown in Fig. 2. A detailed review

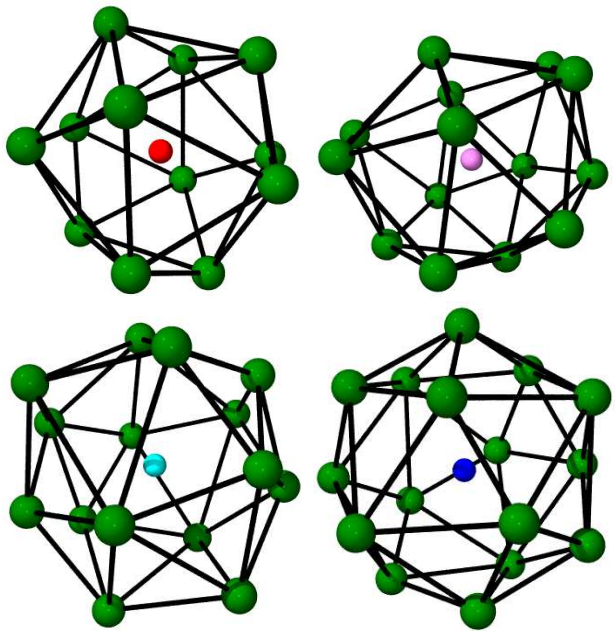

Figure 2: The atoms in topologically close-packed phases are highly coordinated with 12 (upper left) to 16 neighbours (lower right) arranged in regular polyhedra.

on local-coordination polyhedra and their arrangement in networks in *tcp* phases was given by Sinha [5]. Whether a particular polyhedron stabilizes a *tcp* phase depends not only on the interplay with the other polyhedra, but also on the size and band filling fraction of the constituent atoms.

Results

From our compilation of experimentally observed data, we find that the occurrence of the Laves phases C14, C15, and C36 is strongly affected by the difference in atomic size of the two compound elements. To be more precise, at an constant average Mendeleev number $\mathcal{M}_{AB}$, Laves phases with the chemical compositions A_xB_y (with $y > x$) form nearly exclusively with $\mathcal{M}_B > \mathcal{M}_A$, thus

the majority component are the larger atoms. This well known geometric effect is due to the difference in coordination of 12 and 16 between the inequivalent sites, with the latter coordination polyhedra being strongly preferred by the larger atoms. In contrast, the occurrence of the other predominantly observed *tcp* phases A15, μ, σ, and χ exhibits a peak at an average Mendeleev number $\mathcal{M}$ of approximately 58 (Fig. 1). This corresponds to a half-full d-band, consistent with previous observations (see e.g. Ref. [5]). The A15 structures (AB_3) are observed mainly

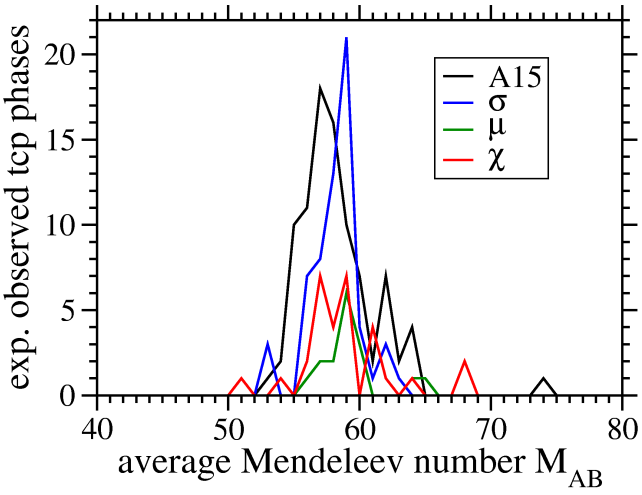

Figure 3: The *tcp* phases A15, σ, μ, and χ in binary transition-metal compounds occur predominantly at an average Mendeleev number $\mathcal{M}$ of 58 that corresponds to a half-full d-band. The Laves phases C14, C15, and C36 (not shown here) are strongly affected by size effects.

for $\mathcal{M}_B < \mathcal{M}_A$ (the smaller atoms form the majority component) and therefore exhibit an interplay of atomic size and electronic effects. The μ, σ, and χ phase are dominated mainly by the average Mendeleev number $\mathcal{M}_{\mathcal{AB}}$. The occurrence of *tcp* phases at half-full d-band coincides with the transition from *bcc* to *hcp* in the structural trend across the 4d and 5d series. In the next section we present DFT calculations for binary compounds of transition metals on either side of this structural transition.

DFT Calculations

The self-consistent density-functional theory calculations presented in this section focus on three compound systems at the structural transition from *bcc* to *hcp* in the 4d and 5d transition-metal series: Re-W, Mo-Re, and Mo-W. For each binary compound, we investigated the *tcp* phases A15, C14, C15, C36, μ, σ, and χ in all possible occupations of the inequivalent sites within the primitive unit-cell. Distributing the atoms in the unit cell without breaking the crystal symmetry results in several crystal structures for each *tcp* phase (e.g., 32 for the σ phase). Additionally, we included more than 40 ordered and disordered fcc and *bcc* based structures. The calculations have been performed using the ab-initio total-energy and molecular-dynamics program VASP (Vienna ab-initio simulation package) developed at the Institut für Materialphysik of the Universität Wien [12, 13, 14]. We employed the projector-augmented waves (PAW) method with the local-density approximation (LDA) to the exchange-correlation functional and pseudo-potentials that treat the outermost p electrons as valence states. We successfully performed convergence tests with respect to the number of plane waves and the **k**-point density. In particular, we found that an energy cutoff of 400 eV and a **k**-point density of 0.02 $(\text{Å}/2\pi)^3$ was sufficient to achieve an accuracy of 1 meV/atom for the cohesive energies. The structural relaxations (of unit cell and internal degrees of freedom) were converged to a maximum force of less than 1 meV/Å. The results presented in the following correspond to the structural stability at a temperature of 0 K. At finite temperatures the occupancy of the individual sites may vary strongly, as was shown for the Re-W σ phase [15] and the Ni-Nb μ phase [16] previously.

Re-W

The system Re-W is of particular interest as it exhibits a rich phase-diagram including σ and χ, but negligible size effects (see e.g. Ref. [15]). The heat of formation for the various structures as obtained from our DFT calculations are compiled in Fig. 4. (We show only the convex hull for each structure type as obtained from our set of DFT calculations.) Our results are in very good agreement with previous DFT calculations of the Re-W σ phase [15]. We find that all the binary *tcp* phases that we considered have a positive heat of formation and are therefore unstable against phase separation to Re (*hcp*) and W (*bcc*), regardless of their chemical composition. Our results are in good quantitative agreement with previous DFT calculations of elemental Re and W structures (cf. Fig. 1(b) in Ref. [17]). The formation energies as obtained from our calculations are well below 50 meV/atom for the A15, σ, and χ phase at chemical compositions of approximately $\text{Re}_{0.33}\text{W}$, $\text{Re}_{0.3-0.5}\text{W}$, and $\text{Re}_{0.6-0.9}\text{W}$,

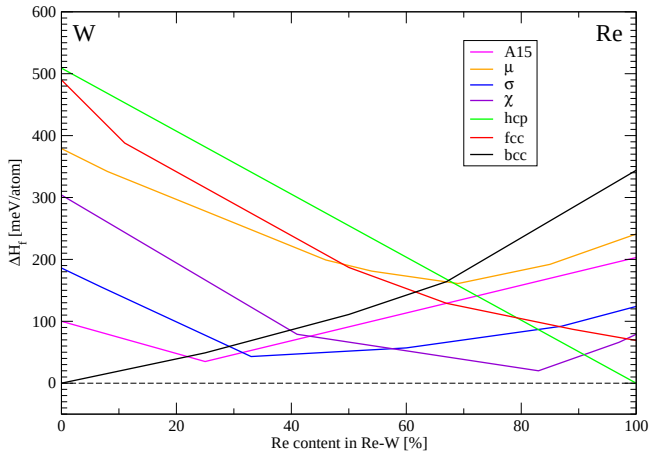

Figure 4: The heat-of-formation diagram of the Re-W system from our DFT calculations shows small positive values for the *tcp* phases A15 (purple), σ (blue), and χ (violet) near the transition from *bcc* (black) to *hcp* (green).

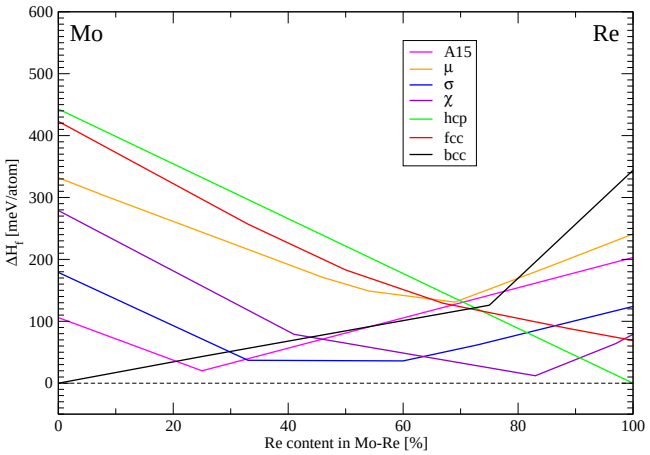

Figure 5: The heat-of-formation diagram of the Mo-Re system obtained by DFT calculations is very similar to the Re-W system (Fig. 4) with small positive values of the *tcp* phases A15 (purple), σ (blue), and χ (violet) near the transition from *bcc* (black) to *hcp* (green).

respectively. These stoichiometries are in line with the experimentally observed σ and χ phase for $Re_{0.43-0.65}W$, $Re_{0.7-0.75}W$ at temperatures of more than 1500 K. In contrast to the σ and χ phase, the A15 structure is not observed experimentally, although we find very similar (positive) heat of formation. This suggests that the entropic contributions to the free energy that stabilize σ and χ at elevated temperatures are less important in the case of A15. The results of our total energy DFT calculations could be employed to investigate the thermodynamic stability of *tcp* phases at finite temperatures by calculating the Gibbs free energy. Whilst the configurational entropy is directly related to the crystal structure (see e.g. Ref. [18]), the calculation of the vibrational entropy would require further, computationally expensive DFT calculations (see e.g. Ref. [19]) that are beyond the scope of this current paper.

Mo-Re

The compound Mo-Re is very similar to Re-W with respect to atomic sizes, average Mendeleev number $\mathcal{M}_{AB}$, and the structural transition from *bcc* to *hcp*. Consequently, the heat of formation for the different structures as obtained from our DFT calculations are nearly identical (Fig. 5). The small positive value of the heat of formation for the σ and χ phase is in line with experimental phase diagrams that observe these phases for similar Re-rich chemical compositions at elevated temperatures. Again, the entropic contributions to the free energy in the case of A15 seem to be too small to stabilize this structure.

Mo-W

The Mo-W system is of particular interest in this study as it is very similar to Re-W and Mo-Re with respect to atomic sizes and the average Mendeleev number $\mathcal{M}_{AB}$. However, both elements form in the *bcc* structure, therefore we do not expect a structural transition in the phase diagram. Our DFT calculations confirm this expectation, the convex hull of all structures show negligible bowing and no intersections (Fig. 6). The *tcp* phases are unstable against phase separation by more than 100 meV/atom for all chemical compositions. We therefore do not expect *tcp* phases to form in the Mo-W system, although the average Mendeleev number would be in the range of *tcp* formation.

Tight-Binding Approximation and Bond-Order Potential

The DFT calculations presented in the previous section can hardly be extended to study trends across all possible binary combinations of transition metals due to the shear

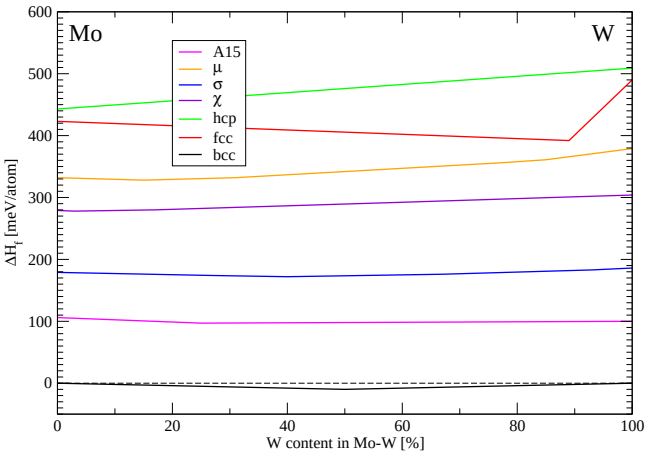

Figure 6: The heat-of-formation diagram of the Mo-W system as obtained from DFT calculations show large formation energies of the *tcp* phases for all chemical compositions.

amount of CPU time required. Therefore, we coarse-grain the description of the electronic structure and continue our study with the tight-binding bond model [20] that has proven to be sufficient for identifying structural trends (see e.g. Refs. [3, 9]).

Formalism

In the non-magnetic d-band tight-binding bond-model the energy is given as a sum of repulsive and bond energies

$$U = U^{\mathrm{rep}} + U^{\mathrm{bond}} \tag{1}$$

where U^{rep} is a pairwise contribution. The bond energy can be given in terms of the electronic density of states $n_{i\alpha}(E)$ of orbital α on atom i as

$$U^{\mathrm{bond}} = \sum_{i\alpha} \int^{E_{\mathrm{F}}} (E - E_i) n_{i\alpha} \mathrm{d}E, \tag{2}$$

or, equivalently, in terms of the density matrix $\rho_{i\alpha j\beta}$ as

$$U^{\mathrm{bond}} = \sum_{i \neq j} \sum_{\alpha\beta} 2\rho_{j\beta i\alpha} H_{i\alpha j\beta}. \tag{3}$$

The density matrix $\rho_{j\beta i\alpha}$ is directly related to the bond order

$$\theta_{j\beta i\alpha} = 2\rho_{j\beta i\alpha} \tag{4}$$

that measures the strength of a bond. Within the bond-order potential (BOP) formalism, the tight-binding DOS is represented as an analytic expansion [3] in terms of moments $\mu_{i\alpha}^{(n)}$

$$\mu_{i\alpha}^{(n)} = \int E^n n_{i\alpha}(E) \mathrm{d}E. \tag{5}$$

that directly relate the local atomic environment to the electronic structure. The derivation of the analytic BOP is based on Chebyshev polynomials of the second kind and presented in detail in Ref. [3]. This BOP depends explicitly on the valence (i.e. the number of valence d electrons per atom) of the transition-metal elements and contains the second-moment Finnis-Sinclair potential at the lowest-order of approximation.

By taking into account the contribution of six moments to the DOS, the analytic BOP reproduces the structural trend from *hcp* to *bcc* to *hcp* to *fcc* across the non-magnetic $4d$ and $5d$ transition metal series. This level of approximation is also sufficient to resolve the structural energy differences of *tcp* phases [2]. In this work we apply the analytic BOP to the structural stability of transition metals in the *tcp* structures A15, C14, C15, C36, σ, and μ. We have implemented the analytic BOP in a multi-purpose modeling package that can also be used for performing structural relaxation and molecular-dynamic simulations.

Structural Trends

Similarly to our previous work on the structural trends across the transition metals [3], we determined the density of states for topologically-close packed phases within the sixth moment approximation of the analytic BOP. In particular, we used canonical nearest-neighbour bond integrals [21]

$$dd\sigma : dd\pi : dd\delta = -6 : 4 : -1 \tag{6}$$

with a decay $\propto 1/R^5$ and band-widths as obtained from tight-binding calculations. The second moment $\mu^{(2)}$ was chosen identical for all structures to guarantee that the structural energy differences are to first order given by the differences in bonding energy [8]. The resulting valence-dependent bond energies shown in Fig. 7 were normalized to the corresponding values of an *fcc* structure at half-full band. The χ phase was not included in this BOP study, because it consists of distorted polyhedra that would require site-dependent cutoff radii for the tight-binding overlap integrals. These results obtained with a sixth-moment approximation of the BOP are in good

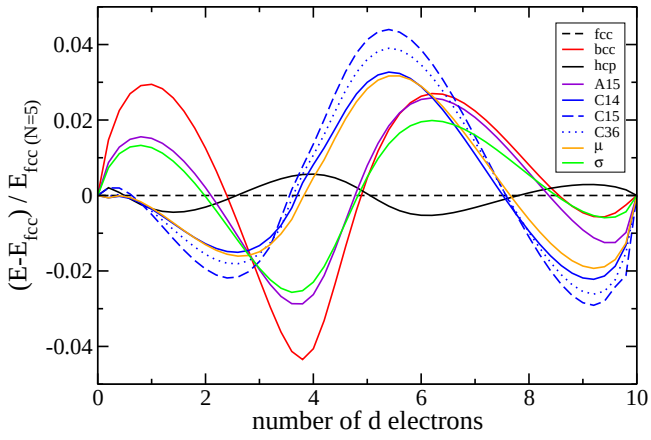

Figure 7: The structural energy differences of *tcp* phases as obtained with the analytic BOP using show that the A15 and σ phase have small positive heat of formation at half-full d-band.

agreement with tight-binding reference calculations that are based on the identical Hamiltonian $H_{i\alpha j\beta}$ of Eq. 3. The structural trend of fcc, bcc, and hcp was already discussed in Ref. [3]. From our new calculations, we find two groups of *tcp* phases that exhibit very similar dependence on the d-band filling: A15 and σ on one hand and μ, C14, C15, and C36 on the other hand. The latter are stabilized by the electronic structure for $N \lessapprox 3$ and $N \gtrapprox 8$. However, our structure map and previous observations (see e.g. Ref. [6]) indicate that the structural stability of the Laves phases is governed by atomic size and packing ratio. In contrast, the electronic structure plays an important role in the stabilization of A15 and σ at the structural transitions from *hcp* to *bcc* at a d-band filling of $N \approx 3$ and from *bcc* to *hcp* at a half-full d-band ($N \approx 5$). The phase competition in the latter regime has also been suggested by previous DFT calculations for unary *tcp* phases of $4d$ and $5d$ TMs by Berne and co-workers [17]. Our DFT calculations for the binary systems Re-W and Mo-Re correspond to intermediate values of the average d-band filling per atom. The phase competition that our BOP predicts in this regime of about half-full d-band is consistent with the small positive values of the heat of formation that we observed in our DFT calculations for the A15 and σ phase of Re-W and Mo-Re. Our BOP results show that a shift of the average d-band filling, e.g., by replacing Re-W with Ru-W, leads to a destabilisation of the *tcp* phases.

Conclusion

In this work we provide a study of the structural stability of topologically close-packed phases by a combination of complimentary approaches: a phenomenological structure map, DFT calculations of particular systems, and bond-order potential calculations of trends across the d-band.

A histogram of experimentally observed *tcp* phases shows the predominant occurrence of the A15, σ, μ, and χ phase at half-full d-band. We performed detailed density-functional theory calculations for the systems Re-W, Mo-Re, and Mo-W with similar d-band filling fraction. The minima of the calculated heats of formations are consistent with the chemical compositions of *tcp* phases in experimental phase diagrams at elevated temperatures. However, the positive values of the formation energies in the range of approximately 50 meV/atom suggest that entropic contributions to the free energy play an important role in the structural stability of binary TCP phases. In order to move beyond the DFT focus on the half-full d-band to the structural trend across the complete transition-metal series, we coarse-grain the description of the electronic structure to the tight-binding bond model, and even further to a recently developed analytic bond-order potential. A comparison with conventional tight-binding calculations based on the same Hamiltonian show that approximating the tight-binding DOS to the level of six moments in the BOP is sufficient to resolve the differences in the bond energy of *tcp* phases. The structural energy differences across the d-band suggest two groups of *tcp* phases with similar behavior. The μ, C14, C15, and C36 phases are stabilized by the bond energy for $N \lessapprox 3$ and $N \gtrapprox 8$. However, the effects of atomic size and packing ratio that govern the stability of these phases are not included in this study. The A15 and σ phase are competing with *hcp* and *bcc* near $N \approx 3$ and with *bcc* and *hcp* at a half-full d-band ($N \approx 5$). The phase competition in the latter regime is in line with our DFT calculations for Re-W and Mo-Re.

We are currently using our DFT results in the parameterization of the analytic BOP. We then plan to use the BOPs to model complex structures and processes that are beyond the scope of present day ab-initio methods, such as the dependence of interface and defect energies on local chemical composition and strain, as well as the kinetic processes of *tcp* formation.

Acknowledgments

We are grateful to M. Sluiter and our collaboration partners in the *Alloys By Design* consortium for many helpful discussions. This work was funded by the Engineering and Physical Sciences Research Council (EPSRC) of the United Kingdom.

References

[1] C.M.F. Rae and R.C. Reed, " The precipitation of topologically close-packed phases in Rhenium-containing superalloys," *Acta mater.* 49, 4113 (2001)

[2] P.E.A. Turchi, "Interplay between local environment effect and electronic structure properties in close packed structures," *Mat. Res. Soc. Symp. Proc.* 206, 265 (1991)

[3] R. Drautz and D.G. Pettifor, "Valence-dependent analytic bond-order potential for transition metals," *Phys. Rev. B* 74, 174117 (2006)

[4] C.M.F. Rae, M.S. Hook, and R.C. Reed, "The effect of *tcp* morphology on the development of aluminide coated superalloys," *Mater. Sci. Eng. A* 396, 231 (2005)

[5] A.K. Sinha, "Topologically close-packed structures of transition metal alloys," *Prog. Mater. Sci.* 15, 79 (1973)

[6] F. Stein, M. Palm, and G. Sauthoff, "Structure and stability of Laves phases. Part I. Critical assessment of factors controlling Laves phase stability," *Intermetallics*, 12, 713 (2004)

[7] D.G. Pettifor, in *Physical Metallurgy*, edited by R.W. Cahn and P. Haasen (Elsevier-North Holland, Amsterdam, 1983), 3rd. ed., and references therein

[8] D.G. Pettifor, *Bonding and Structure of Molecules and Solids* (Oxford University Press, Oxford, 1995)

[9] D.G. Pettifor and R. Podloucky, "The structures of binary compounds: II. Theory of the *pd*-bonded AB compounds," *J. Phys. C: Solid State Phys.* 19, 315 (1986)

[10] W.B. Pearson, *Pearson's handbook of crystallographic data for intermetallic phases*, edited by P. Villars and L.D. Calvert (American Society for Metals, Metals Park, 1985)

[11] Inorganic Crystal Structure Database (ICSD), http://www.icsd.org

[12] G. Kresse and J. Hafner, "Ab-initio molecular-dynamics for liquid-metals," *Phys. Rev. B* 47, 558 (1993); ibid 49, 14251 (1994)

[13] G. Kresse and J. Furthmüller ," Efficiency of ab-initio total energy calculation for metals and semiconductors using a plane-wave basis set," *Comput. Mater. Sci.* 6, 15 (1996)

[14] G. Kresse and G. Furthmüller, "Efficient iterative schemes for ab initio total-energy calculations using a plane-wave basis set," *Phys. Rev. B* 54, 11169 (1996)

[15] C. Berne, M. Sluiter, Y. Kawazoe, T. Hansen, and A. Pasturel, "Site occupancy in the Re-W sigma phase," *Phys. Rev. B* 64, 144103 (2001)

[16] M. Sluiter, A. Pasturel, and Y. Kawazoe, "Site occupation in the Ni-Nb μ phase," *Phys. Rev. B* 67, 174203 (2003)

[17] C. Berne, A. Pasturel, M. Sluiter, and B. Vinet, "Ab Initio Study of Metastability in Refractory Metal Based Systems," *Phys. Rev. Lett.* 83, 1621 (1999)

[18] S.G. Fries and B. Sundman, "Using Re-W σ-phase first-principles results in the Bragg-Williams approximation to calculate finite-temperature thermodynamic properties," *Phys. Rev. B* 66, 012203 (2002)

[19] C. Wolverton and V. Ozoliņš, "Entropically favored ordering: The metallurgy of Al_2Cu revisited," *Phys. Rev. Lett.* 86, 5518 (2001)

[20] A.P. Sutton, M.W. Finnis, D.G. Pettifor, and Y. Ohta, "The tight-binding bond model," *J. Phys. C* 21, 35 (1988)

[21] O.K. Andersen, W. Klose, and H. Nohl, "Electronic structure of Chevrel-phase high-critical-field superconductors," *Phys. Rev. B* 17, 1209 (1978)